

# Aharonov-Bohm effect and Resonances in the circular quantum billiard with two leads

Suhan Ree and L.E. Reichl

*Center for Studies in Statistical Mechanics and Complex Systems  
The University of Texas at Austin, Austin, Texas 78712*

(August 31, 1998)

We calculate the conductance through a circular quantum billiard with two leads and a point magnetic flux at the center. The boundary element method is used to solve the Schrödinger equation of the scattering problem, and the Landauer formula is used to calculate the conductance from the transmission coefficients. We use two different shapes of leads, straight and conic, and find that the conductance is affected by lead geometry, the relative positions of the leads and the magnetic flux. The Aharonov-Bohm effect can be seen from shifts and splittings of fluctuations. When the flux is equal to  $h/2e$  and the angle between leads is  $180^\circ$ , the conductance tends to be suppressed to zero in the low energy range due to the Aharonov-Bohm effect.

PACS numbers: 05.45.+b, 03.65.Ge, 02.70.Pt

Submitted to Phys. Rev. B

## I. Introduction

Aharonov and Bohm, in their historic 1959 paper[1], showed theoretically that charged matter waves are phase shifted if they pass through a magnetic vector potential even when there is no magnetic field present in that region of space. This so-called Aharonov-Bohm effect (AB effect) is a purely quantum mechanical phenomenon. The magnetic vector potential has no effect on classical particles. The AB effect has been observed in several experiments using electron interferometry[2].

The AB effect can also be studied in confined geometries with leads by looking at behaviors of electron transport through these systems. An one-dimensional structure such as a small metal ring with a confined magnetic flux has been used to investigate the connection between the conductance oscillations and the AB effect[3]-[6]. Recent developments in micrometer-scale technology have also made possible new ways to observe the electron transport through confined two-dimensional cavities. These ballistic electron waveguides are formed from the two-dimensional electron gas (2 DEG) found at the interface of GaAs/AlGaAs heterostructure[7]. They are formed at very low-temperature and with sizes of less than  $\mu\text{m}$  to make electrons phase-coherent inside. Since the quantum mechanics can be used to explain the behavior of electrons, these devices also provide a natural place to look for the AB effect[8]-[11].

In these systems, the magnetoresistance has been observed to oscillate with a period of  $h/e$  or  $h/2e$  as the magnetic flux is varied. In the ballistic regime,  $h/e$  oscillation is expected due to gauge invariance in the quantum mechanics. In the diffusive regime (when both the elastic mean free path and the phase-coherence length are not larger than the size of the sample), oscillations

with period  $h/2e$  were observed, and had been predicted theoretically[12]. Kawabata and Nakamura[13] argued that  $h/2e$  oscillation is theoretically predicted even in ballistic cases using the semiclassical scattering theory.

In this paper, we study the conductance properties of a two-dimensional ballistic circular billiard with two leads attached. Circular billiards have been studied before in several contexts. Lin[14] calculated the conductance for this system using the semiclassical conductance formula. In Refs.[15] and [16], circular billiards with two leads were investigated with a homogeneous magnetic field applied. We will apply a point magnetic flux at the center of the circular billiard (AB billiard). Then the cavity contains only the vector potential with no magnetic field. In the system we consider here, the size of the cavity and the temperature are small enough to make the system ballistic, the boundary is formed by a hard-wall potential, and electron-electron interaction is ignored. Under these conditions, the Landauer formula[17]-[19] for two leads can be used to obtain the conductance of the system. (Because  $h/e$  oscillation is expected in this ballistic model, we will only look at the magnetic flux between  $-h/2e$  and  $h/2e$ .) In addition to considering the effect of the vector potential on conductance, we will also consider the effect of the shape of the leads on conductance, and investigate conductance for two different shapes of leads, straight and conic (see Fig. 1). We will find that the shape of the leads and the relative position of leads can have an important effect on the conductance. We will also find that the AB effect can dominate the system under a special circumstance.

In Sec. II, we first consider the properties of eigenstates of a closed circular billiard with a magnetic flux line down its center. In Sec. III, the open billiard is studied, and the boundary element method which is used to

obtain the conductance is discussed. In Sec. IV, we show our numerical results. Finally, we summarize in Sec. V.

## II. Closed Billiard

In this section, we obtain the energy levels for an electron in a closed circular billiard with a magnetic flux line down the center. Reimann *et al.*[20] calculated the energy density of states semiclassically using the Gutzwiller's trace formula. In this paper, we must understand this system quantum mechanically in order to properly interpret the behavior of the open billiard with leads attached in the low energy range. In Ref. [21], we studied this closed system when the flux line oscillates periodically in time. Then magnetic and electric field are induced in the cavity and the system can undergo a transition to chaos. When the flux line is constant in time, only a magnetic vector potential appears in the cavity and there is no chaos but we can study the AB effect.

The Hamiltonian of the system can be written

$$\hat{H}_0(\hat{r}, \hat{p}_r, \hat{p}_\theta) = \frac{\hat{p}_r^2}{2m} + \frac{(\hat{p}_\theta - \alpha\hbar)^2}{2m\hat{r}^2} + \hat{V}_R(\hat{r}), \quad (1)$$

where  $\alpha = \Phi/\Phi_0$  is a dimensionless quantity when  $\Phi$  is the magnitude of the magnetic flux through the center of the cavity and  $\Phi_0 = h/e$ , and  $\hat{V}_R(\hat{r})$  is a hard-wall potential confining the electron to the interior of a circular billiard of radius  $R$ . From here on, we will only consider  $\alpha$  in the range  $-0.5 < \alpha \leq 0.5$ , which is sufficient because of gauge invariance. For  $\alpha = 0$  and  $\alpha = 0.5$ , the energy eigenvalues are two-fold degenerate. However, the flux breaks the time-reversal symmetry of the system when  $0 < |\alpha| < 0.5$ , and removes these two-fold degeneracies. After solving the time-independent Schrödinger equation,  $\hat{H}_0(\alpha)|l, n; \alpha\rangle = E_{ln}(\alpha)|l, n; \alpha\rangle$ , we can find energy eigenstates,

$$\langle r, \theta | l, n; \alpha \rangle = J_{|l-\alpha|} \left( \frac{\beta_{ln}(\alpha)r}{R} \right) e^{il\theta}, \quad (2)$$

and energy eigenvalues,

$$E_{ln}(\alpha) = \frac{\hbar^2 \beta_{ln}(\alpha)^2}{2mR^2}, \quad (3)$$

where  $m$  is the mass of the electron, and  $\beta_{ln}(\alpha)$  is the  $n$ th zero of  $J_{|l-\alpha|}(x)$  ( $l$ : integer,  $n$ : positive integer). The energy eigenvalues,  $E_{ln}(\alpha)$ , are plotted in Fig. 2 as a function of  $\alpha$ . We can easily prove that the energies are symmetric in  $\alpha$ . We also see no level-repulsion as expected since this system has no chaos. When  $\alpha = 0$ ,  $|l, n; 0\rangle$  and  $|-l, n; 0\rangle$  are degenerate, and when  $\alpha = 0.5$ ,  $|l, n; 0.5\rangle$  and  $|l-1, n; 0.5\rangle$  are again degenerate.

## III. Open Billiard

We now create an open system by attaching two infinite leads to the circular AB billiard. As shown in Fig. 1, we

will study two different lead geometries. For one geometry, the leads are straight. For the other geometry, the leads have conic shape. For both geometries, there are four dimensionless quantities which characterize the system. There are two geometric parameters,  $\Delta$  (the opening angle of leads) and  $\gamma$  (the relative angle between leads). There are two physical quantities,  $\alpha = \Phi/\Phi_0$  (the dimensionless magnetic flux) and  $\epsilon = (mR^2/\hbar^2)E_F$  (the dimensionless Fermi energy).

For straight leads, we can calculate the number of propagating modes if we are given values for  $\Delta$  and  $\epsilon$ . If we define the Fermi wave number as  $k_F = \sqrt{2mE_F}/\hbar$ , there are  $n$  propagating modes if

$$\frac{n\pi}{W} \leq k_F < \frac{(n+1)\pi}{W}, \quad (4)$$

where  $W = 2R \sin(\Delta/2)$ . In other words, if  $\epsilon_n \leq \epsilon < \epsilon_{n+1}$ , then there are  $n$  propagating modes in leads where  $\epsilon_n$  is defined as

$$\epsilon_n = \frac{n^2\pi^2}{8\sin^2(\frac{1}{2}\Delta)}. \quad (5)$$

All the remaining modes are evanescent modes. Here we are interested in the energy range,  $\epsilon_0 \leq \epsilon < \epsilon_2$ .

For conic leads, there is no way to distinguish between propagating and evanescent modes before solving the problem, because all existing modes are propagating modes. But, after solving the equation, we find that, except for a finite number of lowest modes, all higher modes will be reflected completely. As we will see in our subsequent results, transmission is not necessarily zero when  $\epsilon < \epsilon_1$  for conical leads, and the second propagating mode starts to transmit when  $\epsilon$  is lower than  $\epsilon_2$ . We will call this "tunneling." The two lead geometries give similar results except for this tunneling effect.

We will briefly look at the numerical method. The partial differential equation we are solving is a Helmholtz equation,

$$(\nabla^2 + k_F^2) \Psi(r, \theta) = 0, \quad (6)$$

with the boundary condition,  $\Psi|_{\text{on all boundaries}} = 0$ . The boundary element method[22, 23] is used to solve this problem. We define a loop  $C$  consisting of two circular segments,  $P_1$  and  $P_2$ , and two segments,  $C_1$  and  $C_2$  across the contacts between the cavity and leads (see Fig. 1). For straight leads,  $C_1$  and  $C_2$  are linear segments, but for conic leads they are parts of a circle, making  $C$  a complete circle. The loop  $C$  divides the whole region into three parts consisting of the interior of the circular cavity, the lead I, and the lead II. We will denote basis states for the interior of the circular cavity by  $\{\phi_l^{(c)} | l : \text{integer}\}$ ; for lead I,  $\{\phi_{n_1}^{(1)\pm} | n_1 \geq 1\}$ ; and for lead II,  $\{\phi_{n_2}^{(1)\pm} | n_2 \geq 1\}$ ; where  $+$  ( $-$ ) stands for an outgoing (incoming) mode. All basis states satisfy the Helmholtz equation. For example,

$$(\nabla^2 + k_F^2) \phi_l^{(c)}(r, \theta) = 0, \quad (7)$$

and so on. For both lead geometries,  $\phi_l^{(c)}$  is given by

$$\phi_l^{(c)}(r, \theta) = c_l^{(c)} J_{|l-\alpha|}(k_F r) e^{il\theta}. \quad (8)$$

For the straight leads, we have

$$\phi_{n_i}^{(i)\pm}(x_i, y_i) = \begin{cases} c_{n_i}^{(i)} \sin(n_i \pi y_i / W) e^{\pm i k_{n_i} x_i} & (1 \leq n_i \leq N_p); \\ c_{n_i}^{(i)} \sin(n_i \pi y_i / W) e^{-\kappa_{n_i} x_i} & (N_p < n_i), \end{cases} \quad (9)$$

where  $(x_i, y_i)$ 's are local coordinates,  $k_{n_i} = \sqrt{(2m/\hbar^2)E_F - (n_i^2 \pi^2 / W)^2}$ , and  $\kappa_{n_i} = \sqrt{(n_i^2 \pi^2 / W)^2 - (2m/\hbar^2)E_F}$ . (In this case,  $\alpha$  is set to zero inside the leads as an approximation to simplify the bases.  $i = 1, 2$ .) We have  $N_p$  propagating modes where  $N_p$  is the largest integer  $n$  satisfying  $(n^2 \pi^2 / W)^2 \leq (2m/\hbar^2)E_F$ .

For the conic leads, we have

$$\phi_{n_i}^{(i)+}(r_i, \theta_i) = c_{n_i}^{(i)} H_{n_i \pi / \Delta}^{(2)}(k_F r_i) \sin\left(\frac{n_i \pi \theta_i}{\Delta}\right) e^{i\alpha \theta_i}, \quad (10)$$

and

$$\phi_{n_i}^{(i)-}(r_i, \theta_i) = c_{n_i}^{(i)} H_{n_i \pi / \Delta}^{(1)}(k_F r_i) \sin\left(\frac{n_i \pi \theta_i}{\Delta}\right) e^{i\alpha \theta_i}, \quad (11)$$

where  $(r_i, \theta_i)$ 's are local coordinates and  $H_\nu^{(1)}$  and  $H_\nu^{(2)}$  are the Hankel functions ( $i = 1, 2$ ). The normalization constants,  $c_{n_i}^{(i)}$ 's, are chosen to make the incoming flux of electrons unity.

The solution to the Helmholtz equation, Eq. (6), can be expressed as follows. Inside the cavity,

$$\Psi^{(c)}(r, \theta) = \sum_{l=-\infty}^{\infty} a_l \phi_l^{(c)}(r, \theta); \quad (12)$$

in lead I with an incoming wave of  $k$ th mode,

$$\Psi^{(1)}(r_1, \theta_1) = \phi_k^{(1)-}(r_1, \theta_1) + \sum_{j=1}^{\infty} r_{jk} \phi_j^{(1)+}(r_1, \theta_1); \quad (13)$$

and in lead II,

$$\Psi^{(2)}(r_2, \theta_2) = \sum_{j=1}^{\infty} t_{jk} \phi_j^{(2)+}(r_2, \theta_2), \quad (14)$$

where  $r_{jk}$  and  $t_{jk}$  are reflection and transmission amplitudes, respectively.

Let us now consider the boundary conditions on loop  $C$ . (The boundary conditions on the walls of leads are already taken care of, because the bases we chose in leads satisfy those conditions.) On boundaries  $C_1$  and  $C_2$ , we have the boundary conditions,

$$\Psi^{(c)}|_{\text{on } C_i} = \Psi^{(i)}|_{\text{on } C_i}, \quad (15)$$

and

$$\frac{\partial \Psi^{(c)}}{\partial n} \Big|_{\text{on } C_i} = \frac{\partial \Psi^{(i)}}{\partial n} \Big|_{\text{on } C_i}, \quad (16)$$

where  $n$  is a normal coordinate of boundaries ( $i = 1, 2$ ). To express the boundary condition on  $P_1$  and  $P_2$ , we will introduce bases,  $\{\xi_{\nu_1}^{(1)} | \nu_1 : \text{integer}\}$  and  $\{\xi_{\nu_2}^{(2)} | \nu_2 : \text{integer}\}$ . They are defined on  $P_i$  as

$$\xi_{\nu_i}^{(i)}(\lambda_i) = \frac{1}{\sqrt{\Delta_i}} e^{i \frac{2\nu_i \pi}{\Delta_i} \lambda_i}, \quad (17)$$

where  $\lambda_i$  is a longitudinal coordinate along the boundary  $P_i$  and  $\Delta_i$  is the size of the boundary  $P_i$  ( $i = 1, 2$ ). Then these boundary conditions are written as

$$\Psi^{(c)}|_{\text{on } P_i} = 0, \quad (18)$$

and

$$\frac{\partial \Psi^{(c)}}{\partial n} \Big|_{\text{on } P_i} = \sum_{\nu_i=-\infty}^{\infty} b_{\nu_i}^{(i)} \xi_{\nu_i}^{(i)}. \quad (19)$$

We multiply Eq. (7) by  $\Psi^{(c)}$  and we multiply Eq. (6) by  $\phi_l^{(c)}$ , and subtract one from another. Then, we integrate over the loop  $C$ . From the Green's theorem, we get the equation,

$$\oint_C d\lambda \left[ \Psi^{(c)} \frac{\partial \phi_l^{(c)}}{\partial n} - \frac{\partial \Psi^{(c)}}{\partial n} \phi_l^{(c)} \right] = 0. \quad (20)$$

$\Psi^{(c)}$  and  $\frac{\partial \Psi^{(c)}}{\partial n}$  are obtained using Eqs. (15), (16), (18), and (19). With suitable truncations, after integrating over each segment, we finally obtain a matrix equation  $\mathbf{A} \cdot \mathbf{x} = \mathbf{B}$ . Solving this matrix equation gives us the values for  $r_{ij}$ ,  $t_{ij}$ ,  $b_{\nu_1}^{(1)}$ , and  $b_{\nu_2}^{(2)}$ . ( $a_l$ 's can be obtained using these values following similar steps.)

The reflection and transmission amplitudes,  $r_{ij}$  ( $i, j \leq N_p$ ) and  $t_{ij}$  ( $i, j \leq N_p$ ), respectively, determine the left half of the  $\mathbf{S}$  matrix,

$$\mathbf{S} = \begin{pmatrix} \mathbf{r} & \mathbf{t}' \\ \mathbf{t} & \mathbf{r}' \end{pmatrix}, \quad (21)$$

for the open circular billiard. In Eq. (21),  $\mathbf{r}$ ,  $\mathbf{t}$ ,  $\mathbf{r}'$ , and  $\mathbf{t}'$  are  $(N_p \times N_p)$ -submatrices of  $\mathbf{S}$ , and  $N_p$  is the number of channels in the lead. The quantities  $\mathbf{r}$  and  $\mathbf{t}$  are matrices containing the reflection amplitudes and the transmission amplitudes, respectively, when there is an incoming wave in lead I. Also, the right half of the  $\mathbf{S}$  matrix,  $\mathbf{r}'$  and  $\mathbf{t}'$ , can be obtained by having an incoming wave in the lead II instead of the lead I. But, in our geometries, it can be done by changing the direction of the magnetic flux.

The conductance for this system is obtained from the transmission amplitudes,  $t_{ij}$ , using the Landauer formula. For transmission from lead I to lead II the Landauer formula is given by

$$G_{I \rightarrow II} = \frac{2e^2}{h} \sum_{i,j=1}^{N_p} |t_{ij}|^2. \quad (22)$$

On the other hand, the conductance from lead II to lead I is given by  $G_{II \rightarrow I} = (2e^2/h) \sum_{i,j=1}^{N_p} |t'_{ij}|^2$ . But, in two-lead conductors,  $G_{I \rightarrow II}$  should be equal to  $G_{II \rightarrow I}$  due to the reciprocity of  $\mathbf{S}$  matrix[24].

## IV. Numerical Results

Let us now show some of our results. The value of  $\Delta$  is set to  $20^\circ$  throughout,  $\gamma$  is  $180^\circ$  or  $90^\circ$ . Here  $\epsilon$  is varied from  $\epsilon_0$  to  $\epsilon_2$  where  $\epsilon_0 = 0$ ,  $\epsilon_1 = 40.91$ , and  $\epsilon_2 = 163.7$ . The conductance is calculated using the Landauer formula, Eq. (22). We define the transmission probability  $T_i \equiv \sum_{j=1}^{N_p} |t_{ji}|^2$  ( $i \leq N_p$ ) when there is an  $i$ th incoming wave in lead I. For each  $i$ ,  $T_i + R_i = 1$  is satisfied due to the unitarity of the  $\mathbf{S}$  matrix when  $R_i = \sum_{j=1}^{N_p} |r_{ji}|^2$ . Then the conductance from lead I to lead II is

$$G_{I \rightarrow II} = \frac{2e^2}{h} \sum_{i=1}^{N_p} T_i. \quad (23)$$

We will compute  $T_1$  and  $T_2$  for  $\epsilon_0 < \epsilon < \epsilon_2$  for the two different lead geometries.

Figure 3 shows our results for the conductance for the case of straight leads for  $\epsilon_0 < \epsilon < \epsilon_2$  when  $\gamma = 180^\circ, 90^\circ$  and  $\alpha = 0, 0.25$ . Only  $T_1$  is plotted versus  $\epsilon$ . Note that for straight leads,  $T_1$  is zero for  $\epsilon < \epsilon_1$ , and  $T_2$  is zero for  $\epsilon < \epsilon_2$ .

Figure 4 shows the analogous results for the case of conic leads for  $\epsilon_0 < \epsilon < \epsilon_2$  when  $\gamma = 180^\circ, 90^\circ$  and  $\alpha = 0, 0.25$ . We see that  $T_1$  ( $T_2$ ) starts to emerge when  $\epsilon$  is lower than  $\epsilon_1$  ( $\epsilon_2$ ). It is useful to note that this case has clear computational advantages. When we integrate over  $C_i$ 's, the Bessel functions are constant, while it is not true in the case of straight leads. As a result, the computation was much faster. Furthermore, we can keep  $\alpha \neq 0$  also in leads by choosing suitable bases in leads without spending more significant computer time.

There are several conclusions we can draw from these results. First, the shape of the lead matters. For the conic leads, the particle can tunnel through the circular cavity at energies which forbid any propagation in the straight leads. On the other hand, away from tunneling energies, both lead geometries give us similar results in the most of the range we looked at.

Second, we can see patterns of fluctuations in all cases in Figs. 3 and 4. They have peaks and valleys. (Most of valleys go down to zero. We will call them "transmission zeros". We believe that valleys (the transmission zeros, in particular) are related to energy eigenvalues of the closed billiard. Although there is no exact one-to-one correspondence, we see loose connections, especially in Figs. 3(b) and 4(b). Therefore, these transmission zeros (which are reflection peaks) can be treated as resonances with the cavity.

Third, our results depend on the relative position of the leads. Although the patterns look similar, we can see

that the locations of peaks and valleys are different for the case  $\gamma = 180^\circ$  and the case  $\gamma = 90^\circ$ . Transmission zeros for the case  $\gamma = 90^\circ$  are more likely to match with energy eigenvalues of the closed billiard (see Figs. 3(b) and 4(b)). This is reasonable because when  $\gamma \neq 180^\circ$ , electrons are more likely to feel the circular billiard.

Fourth, we can see an indirect result of the AB effect. When  $\alpha = 0.25$ , we see almost twice as many fluctuations as when  $\alpha = 0$ . This means that, if we increase  $\alpha$  from zero, fluctuations will split and be shifted at the same time. This is due to the AB effect.

Let us now look at the conductance from another point of view. In Fig. 5, we computed  $G_{I \rightarrow II}$  of the case of conic leads assuming the energy is a complex number. We see a series of poles near the real axis. Such poles have been seen for simple systems relating to transmission zeros [23],[25],[26]. However, we cannot establish an exact correspondence because our conductance curves are too crowded with fluctuations. One interesting feature, however, is the big poles which follow a line across the complex plane when  $\gamma = 180^\circ$  (see Figs. 5(a) and 5(c)). When  $\gamma = 90^\circ$ , Figs. 5(b) and 5(d) show that they become less regularly distributed.

Let us now show our results for the special case of  $\alpha = 0.5$ . In Fig. 6, we show graphs of  $T_1$  and  $T_2$  as a function of  $\epsilon$  for the cases of conic leads when  $\gamma = 180^\circ$  (Fig. 6(a)) and  $\gamma = 90^\circ$  (Fig. 6(b)). The graphs for the cases of straight leads show almost the same results, but are not shown here.

In Fig. 6(b), when  $\gamma = 90^\circ$ , we see the same type of fluctuation pattern that we saw in Figs. 3 and 4. In Fig. 6(a), however, when  $\gamma = 180^\circ$ , we see the shut-down of the conductance in the lower energy range. This can be roughly explained using concepts from the theory of path integrals. The transmission amplitude from lead I to lead II is approximately proportional to the Green's function of Eq. (6) from the point at the center of  $C_1$  to the point at the center of  $C_2$  when  $\Delta$  is small. The propagator can be obtained using the path integral by summing over all paths. These paths can be divided into two groups, upper and lower paths. Since this particular case has the reflection symmetry along an axis parallel to leads, each lower path is the exact mirror image of an upper path, and they cancel each other due to the AB effect only when  $\alpha = 0.5$ . This is destructive quantum interference. If the propagator vanishes, the Green's function vanishes, too. Therefore, the conductance almost vanishes in this case. This is true only when the Fermi wavelength of the electron is comparable to the width of the opening in the lower energy range. As energy gets bigger, this AB effect will be less pronounced because of the finiteness of the width of leads.

## V. Conclusions

In this idealized model, we have calculated the conductance through the circular AB billiard with two leads using the Landauer formula. We have shown that the shape and the relative position of leads can play important roles in transport properties of the open AB billiard. We have observed generic fluctuation patterns, which can be interpreted as resonances. Transmission zeros tend to correspond well with energy eigenvalues of the closed billiard, especially when  $\gamma = 90^\circ$ . We have also calculated the conductance for complex energies, and found regularly located big poles. We have seen the significant AB effect in the special case of  $\gamma = 180^\circ$  and  $\alpha = 0.5$ . Then the conductance was suppressed to zero in the lower part of the energy range we looked at.

## Acknowledgments

The authors wish to thank the Welch Foundation, Grant No.F-1051, NSF Grant No.INT-9602971, and DOE contract No.DE-FG03-94ER14405 for partial support of this work. We thank NPACI and the University of Texas High Performance Computing Center for use of its facilities. The authors also wish to thank Kyungsun Na and Professor German Luna-Acosta for many helpful discussions, and Professor Alex de Lozanne for helpful discussions concerning experiments.

## References

- [1] Y. Aharonov and D. Bohm, Phys. Rev. **115**, 485 (1959)
- [2] A. Tonomura *et al*, Phys. Rev. Lett. **48**, 1443 (1982); G. F. Missiroli, G. Pozzi and U. Valdre, J. Phys. F **14**, 649 (1981)
- [3] M. Büttiker, Y. Imry, and M. Ya. Azbel, Phys. Rev. A **30**, 1982 (1984)
- [4] R. A. Webb, S. Washburn, C. P. Umbach, and R. B. Laibowitz, Phys. Rev. Lett. **54**, 2696 (1985)
- [5] V. Chandrasekhar, M. J. Rooks, S. Wind, and D. E. Prober, Phys. Rev. Lett. **55**, 1610 (1985)
- [6] V. Chandrasekhar, R. A. Webb, M. J. Brady, M. B. Ketchen, W. J. Gallagher, and A. Kleinsasser, Phys. Rev. Lett. **67**, 3578 (1991)
- [7] C. M. Markus, A. J. Rimberg, R. M. Westervelt, P. F. Hopkins, and A. C. Gossard, Phys. Rev. Lett. **69**, 506 (1992)
- [8] S. Datta, M. R. Melloch, S. Bandyopadhyay, R. Noren, M. Vaziri, M. Miller, and R. Reifengerger, Phys. Rev. Lett. **55**, 2344 (1985)
- [9] G. Timp, A. M. Charng, J. E. Cunningham, T. Y. Chang, P. Mankiewich, R. Behringer, and R. E. Howard, Phys. Rev. Lett. **58**, 2814 (1987)
- [10] B. J. van Wees, L. P. Kouwenhoven, C. J. P. M. Harmons, J. G. Williamson, C. E. Timmering, M. E. I. Broekaart, C. T. Foxon, and J. J. Harris, Phys. Rev. Lett. **62**, 2523 (1989)
- [11] A. Yacoby, M. Heiblum, D. Mahalu, and H. Shtrikman, Phys. Rev. Lett. **74**, 4047 (1995); A. Yacoby, R. Schuster, and M. Heiblum, Phys. Rev. B **53**, 9583 (1996)
- [12] B. L. Al'tshuler, A. G. Aronov, and B. Z. Spivak, Pis'ma Zh. Eksp. Teor. Fiz. **33**, 101 (1981) [JETP Lett. **33**, 94 (1981)]
- [13] S. Kawabata and K. Nakamura, Chaos, Solitons & Fractals **8**, 1085 (1997)
- [14] W. A. Lin, Chaos, Solitons & Fractals **8**, 995 (1997)
- [15] M. Persson, J. Pettersson, B. von Sydow, P. E. Lindelof, A. Kristensen, and K. F. Berggren, Phys. Rev. B **52**, 8921 (1995)
- [16] K. F. Berggren, Z. L. Ji, and T. Lundberg, Phys. Rev. B **54**, 11 612 (1996)
- [17] R. Landauer, IBM J. Res. Dev. **1**, 223 (1957)
- [18] A. D. Stone and A. Szafer, IBM J. Res. Dev. **32**, 384 (1988)
- [19] H. U. Baranger and A. D. Stone, Phys. Rev. B **40**, 8169 (1989)
- [20] S. M. Reimann, M. Brack, A. G. Magner, J. Blaschke, and M. V. N. Murthy, Phys. Rev. A **53**, 39 (1996)
- [21] S. Ree and L. E. Reichl, Phys. Rev. E **55**, 2409 (1997)
- [22] H. R. Frohne, M. J. McLennan, and S. Datta, J. Appl. Phys. **66**, 2699 (1989)
- [23] K. Na and L. E. Reichl, "Electron conductance and lifetime in a ballistic electron waveguide," [J. of Stat. Phys. (to be published)]
- [24] M. Büttiker, IBM J. Res. Dev. **32**, 317 (1988)
- [25] F. Bagwell and R. K. Lake, Phys. Rev. B **46**, 15 329 (1992)
- [26] Z. Shao, W. Porod, and C. S. Lent, Phys. Rev. B **49**, 7453 (1994)

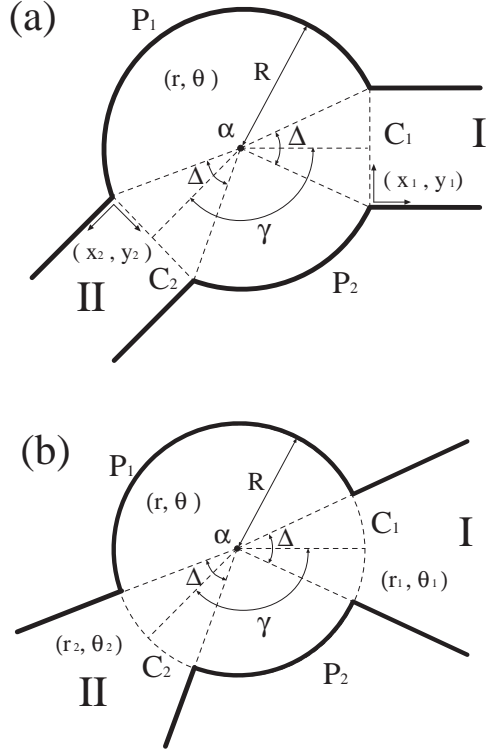


Figure 1: Geometries of two models. (a) Circular AB billiard with two straight leads. (b) Circular AB billiard with two conic leads. In both cases, the magnetic point flux  $\alpha$  is placed at the center.  $R$  is the radius of the billiard,  $\gamma$  is the angle between two leads, and  $\Delta$  is the opening angle of leads.

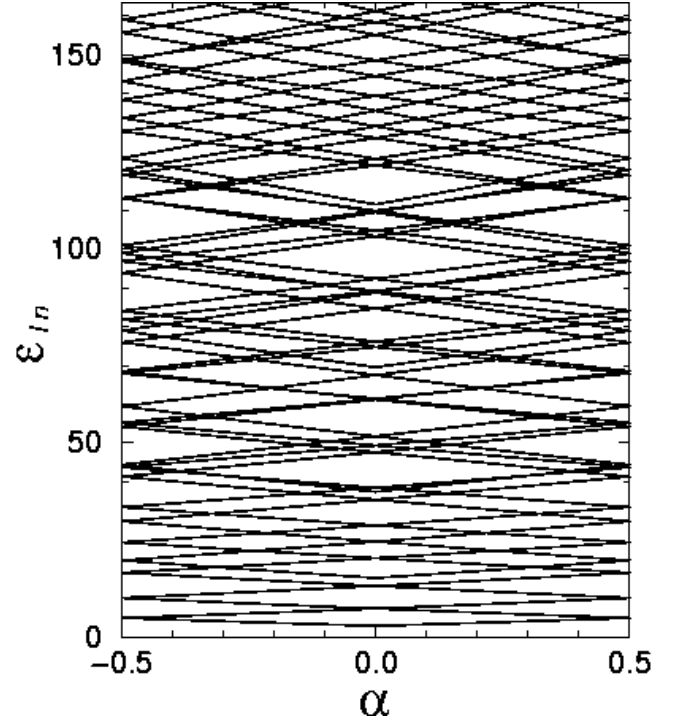


Figure 2: Energy eigenvalues of the closed circular AB billiard as a function of the magnetic flux  $\alpha$  ( $= \Phi/\Phi_0$ ).  $\epsilon_{ln}$  is a dimensionless quantity defined by  $\epsilon_{ln} = (mR^2/\hbar^2) E_{ln}$ .

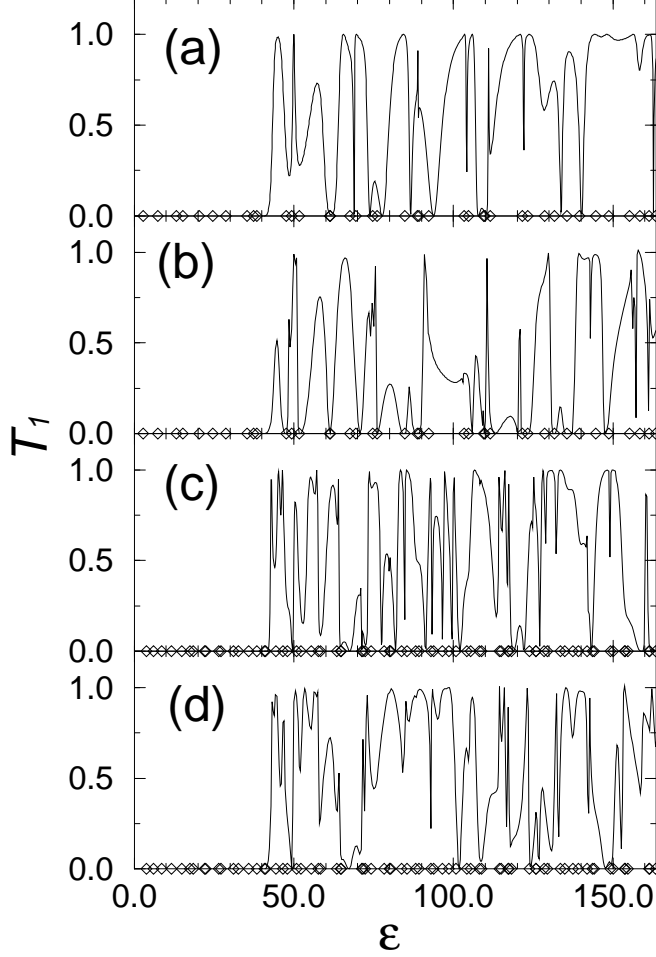


Figure 3:  $T_1$  (transmission probability for the first mode incoming) vs. Fermi energy  $\epsilon$  for the case of straight leads when  $\Delta = 20^\circ$ . (a)  $\alpha = 0, \gamma = 180^\circ$ . (b)  $\alpha = 0, \gamma = 90^\circ$ . (c)  $\alpha = 0.25, \gamma = 180^\circ$ . (d)  $\alpha = 0.25, \gamma = 90^\circ$ . Points( $\diamond$ ) show the energy eigenvalues of the closed AB billiard with corresponding  $\alpha$  value.  $\epsilon = (mR^2/\hbar^2)E_F$ .  $\epsilon$  is in the range of  $\epsilon_0 < \epsilon < \epsilon_2$  where  $\epsilon_0 = 0$ ,  $\epsilon_1 = 40.91$ , and  $\epsilon_2 = 163.7$ .  $T_i (i > 1)$  is equal to zero in this range. The conductance  $G_{I \rightarrow II}$  is obtained from  $(2e^2/h)T_1$ .

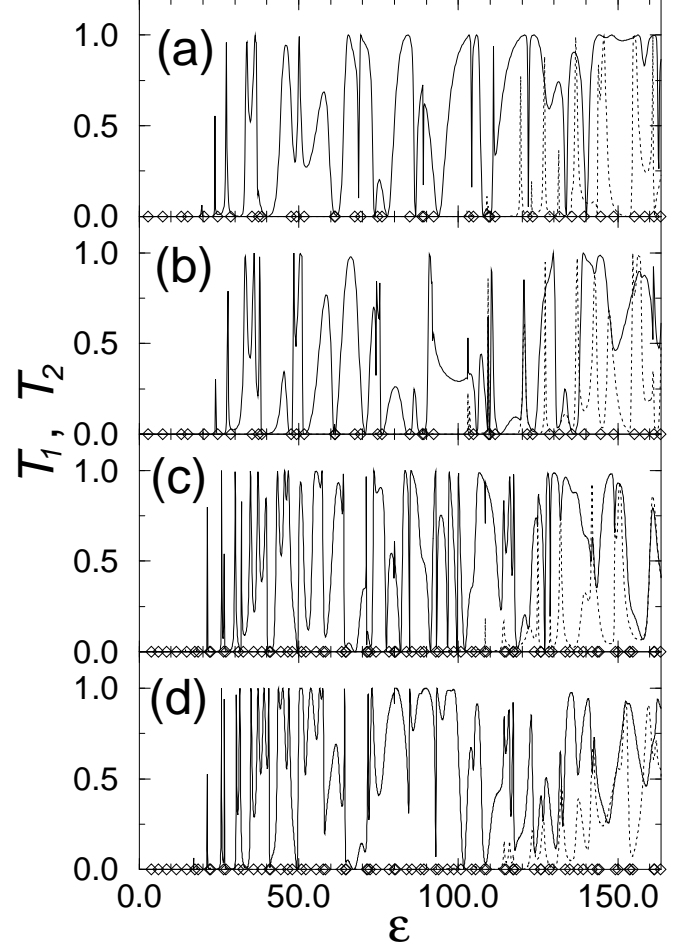


Figure 4:  $T_1$  and  $T_2$  (transmission probability for the first or second mode incoming, respectively) vs. Fermi energy  $\epsilon$  for the case of conic leads when  $\Delta = 20^\circ$ . (a)  $\alpha = 0, \gamma = 180^\circ$ . (b)  $\alpha = 0, \gamma = 90^\circ$ . (c)  $\alpha = 0.25, \gamma = 180^\circ$ . (d)  $\alpha = 0.25, \gamma = 90^\circ$ . Points( $\diamond$ ) show the energy eigenvalues of the closed AB billiard with corresponding  $\alpha$  value.  $T_1$  (solid) starts to emerge before  $\epsilon_1$ , and  $T_2$  (dotted) emerges before  $\epsilon_2$ . The conductance  $G_{I \rightarrow II}$  is obtained from  $(2e^2/h)(T_1 + T_2)$ .

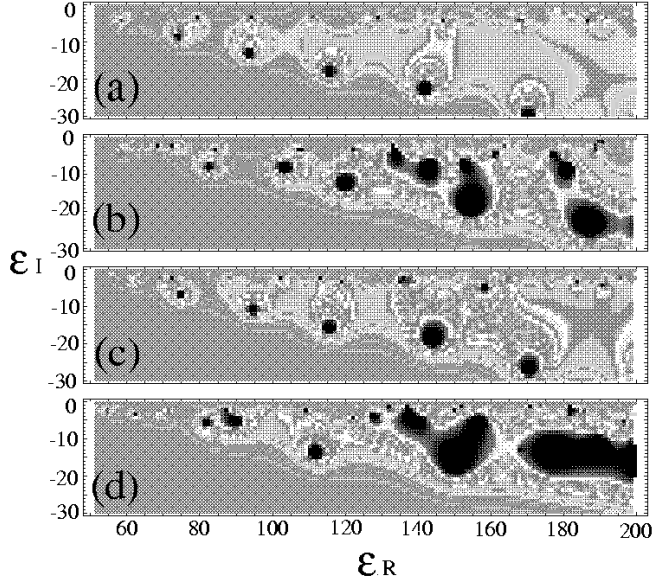


Figure 5: Conductance  $G_{I \rightarrow II}$  vs. complex energy  $\epsilon_R + i\epsilon_I$  for the case of conic leads when  $\Delta = 20^\circ$ . (a)  $\alpha = 0$ ,  $\gamma = 180^\circ$ . (b)  $\alpha = 0$ ,  $\gamma = 90^\circ$ . (c)  $\alpha = 0.25$ ,  $\gamma = 180^\circ$ . (d)  $\alpha = 0.25$ ,  $\gamma = 90^\circ$ . Dark spots represent poles in the complex plane. Small poles near the real axis ( $\epsilon_I = 0$ ) correspond to fluctuations we saw in Fig. 4. But, we also observe big poles marching down regularly.

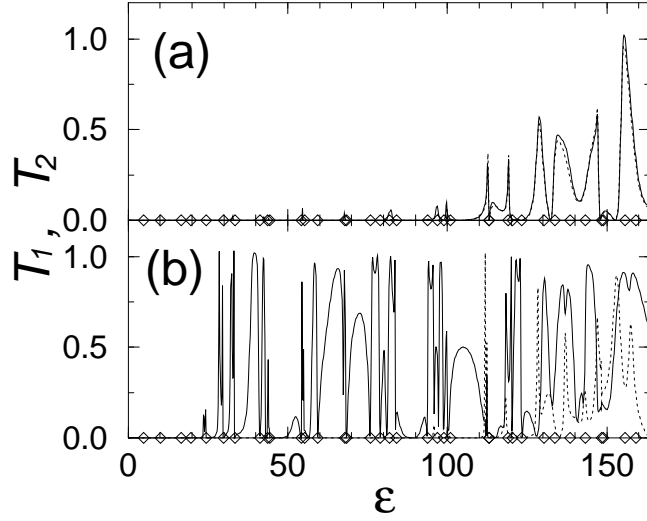


Figure 6:  $T_1$  and  $T_2$  vs. Fermi energy  $\epsilon$  for the case of conic leads when  $\Delta = 20^\circ$  and  $\alpha = 0.5$ . (a)  $\gamma = 180^\circ$ . (b)  $\gamma = 90^\circ$ . Points ( $\diamond$ ) show the energy eigenvalues of the closed AB billiard with  $\alpha = 0.5$ . In (a),  $T_1$  (solid) and  $T_2$  (dotted) are suppressed to zero in the lower region due to the Aharonov-Bohm effect. But, in (b), fluctuations are observed as in Fig. 4.